Upper and Lower Bounds on the Capacity of Wireless Optical Intensity Channels Corrupted by Gaussian Noise

Steve Hranilovic and Frank R. Kschischang
The Edward S. Rogers Sr. Department of Electrical and Computer Engineering
University of Toronto
Email: {steve,frank}@comm.utoronto.ca

Abstract— **This paper finds asymptotically exact upper and lower bounds on the channel capacity of power and band-limited optical intensity channels corrupted by white Gaussian noise. This work differs from the oft investigated case of the Poisson photon counting channel in that not only are rectangular pulse amplitude schemes considered, but general results for all time-disjoint intensity modulation schemes are presented. The role of bandwidth is expressed by way of the effective dimension of the set of signals and together with an average optical power constraint is used to determine bounds on the spectral efficiency of time-disjoint optical intensity signalling schemes. The signal independent, additive white Gaussian noise model is realistic for indoor free-space optical channels. The bounds show that at high optical signal-to-noise ratios the use of bandwidth efficient pulse sets is essential to achieve high spectral efficiencies. This result can be considered as an extension of previous work on photon counting channels which more closely model low optical intensity channels.**

I. Introduction

Previous investigations into the capacity of optical intensity systems has focused primarily on channels in which the dominant noise source is quantum in nature. In these channels the transmitted optical intensity is constant in discrete time intervals. The received signal is modelled by a Poisson distributed count of the number of received photons in each discrete interval. The capacity of such channels has been reported under a variety of peak and average optical power constraints [1–4]. It has also been shown that schemes based on photon counting in discrete intervals require an exponential increase in bandwidth as a function of the rate (in nats/photon) for reliable communication [5].

In this work we present capacity bounds for a fundamentally different optical intensity channel. The indoor free-space optical channel can be modelled as a lowpass, linear channel with additive, white, signal independent, Gaussian noise [6]. Unlike previous treatments, capacity bounds are computed for any time-disjoint modulation scheme under a constraint on the bandwidth of any codeword.

II. The Optical Intensity Channel

Optical intensity channels transmit information by modulating the optical power of a laser or LED light source. Take some optical intensity signal $x(t)$ to be transmitted. The channel which is composed of the multipath response of the room as well the electrical characteristics of the opto-electronics can be modelled by a linear conversion between optical and electrical domains [6]. The transmitted signal is corrupted by noise which can be modelled as being additive white Gaussian distributed [6]. Thus, the received electrical signal, $y(t)$ can be written as

$$y(t) = rx(t) + z(t)$$

where $r > 0$ is the *responsivity* of the photodiode in units of Amperes per Watt and $z(t)$ is zero mean AWGN. Since the transmitted signal is an intensity, $x(t)$ must satisfy $\forall t$ $x(t) \geq 0$. Due to eye and skin safety regulations the average optical power is limited, and hence the average amplitude of $x(t)$ is limited. The received electrical signal $y(t)$ can assume negative amplitude values.

Note that this channel model applies not only to free-space optical channels but also to fiber optic links with negligible dispersion and signal independent, additive, white, Gaussian noise.

III. Signal Space Model

The free-space optical channel can be viewed as a vector channel with respect to the time-disjoint, orthonormal M-dimensional signal basis $\{\phi_1(t), \phi_2(t), \ldots, \phi_M(t)\}$, where $\phi_m(t) = 0$ for $t \notin [0, T)$. The vector channel can then be represented as $\mathbf{Y} = \mathbf{X} + \mathbf{Z}$, where each term is an M-dimensional random vector distributed as $f_{\mathbf{Y}}(\mathbf{y})$, $f_{\mathbf{X}}(\mathbf{x})$ and $f_{\mathbf{Z}}(\mathbf{z})$ respectively where $\mathbf{Z}$ is Gaussian with uncorrelated components. In order to adapt the signal space model to the optical intensity channel, we specify

$$\phi_1(t) = \frac{1}{\sqrt{T}}, \quad t \in [0, T) \tag{1}$$

as a basis function for every intensity modulation scheme [7]. This basis function represents the average amplitude of each symbol, and as a result represents the average optical power of each symbol.

The *admissible region* of the optical intensity modulation scheme is defined as the set of all points in the signal space which describe non-negative pulses, or formally

$$\Upsilon = \left\{ (\upsilon_1, \upsilon_2, \ldots, \upsilon_M) \in \mathbb{R}^M : (\forall t \in \mathbb{R}), \sum_{m=1}^{M} \upsilon_m \phi_m(t) \geq 0 \right\}.$$

This work was supported in part by an Ontario Graduate Scholarship in Science and Technology.

It can be shown that Υ is the convex hull of a generalized N-cone with vertex at the origin [7]. Clearly $f_{\mathbf{X}}(\mathbf{x}) = 0$ for $\mathbf{x} \notin \Upsilon$ to ensure the non-negativity constraint is met. Additionally, since Υ is a generalized cone, it can be parameterized by the coordinate value in the ϕ_1 direction as well as the set of points

$$\Upsilon_k = \{(\upsilon_1, \upsilon_2, \ldots, \upsilon_N) \in \Upsilon : \upsilon_1 = k, k \in \mathbb{R}, k \geq 0\}.$$

The average optical power, P, of an intensity signalling set can then be computed as

$$\begin{aligned} rP &= \frac{1}{\sqrt{T}} \int_{\mathbf{x}\in\Upsilon} x_1 f_{\mathbf{X}}(\mathbf{x}) d\mathbf{x} && (2) \\ &= \frac{1}{\sqrt{T}} P^{\mathsf{G}}, && (3) \end{aligned}$$

where P^{G} is the expected value of the x_1 component of each signal vector and depends solely on $f_{\mathbf{X}}(\mathbf{x})$. Note that the responsivity, r, allows the optical constraints to be cast in terms of electrical quantities. In this case, rP is in units of Amperes.

IV. Upperbound on Channel Capacity

An upper-bound on the capacity of a Gaussian noise corrupted channel can be obtained by considering a sphere-packing argument in the set of all received codewords while imposing an average optical power constraint. This analysis is done in the same spirit as Shannon's sphere packing argument for channels subject to an average electrical power constraint [8]. Determining this bound requires that the volume of the set of received codewords be computed for a given average optical power limit.

A. Set of Transmitted Codewords

Consider transmitting a codeword $\mathbf{x}$ formed from a series of N, M-dimensional symbols at a low probability of error. Geometrically, in order for $\mathbf{x}$ to be transmittable, $\mathbf{x} \in \Upsilon^N$ where Υ^N is the N-fold Cartesian product of Υ with itself. Recall from Section III that Υ is the convex hull of a generalized cone parameterized by the Υ_k cross-sections at $\phi_1 = k$. The Cartesian product Υ^N represents the set of transmittable codewords formed by the concatenation in time of N time-limited symbols. As a result, Υ^N represents a time-limited optical intensity scheme and is the convex hull of a generalized cone with vertex at the origin [7]. In an analogous fashion to (1), define the ϕ_1^{MN} basis vector as

$$\phi_1^{MN} = \frac{1}{\sqrt{N}} \underbrace{(\underbrace{1,0,0,\ldots,0}_{M}, \underbrace{1,0,0,\ldots 0}_{M}, 1,0,0,\ldots)}_{MN} \quad (4)$$

so that it represents the average optical power of each MN-dimensional codeword $\mathbf{x} \in \Upsilon^N$. The region Υ^N is then parameterized by cross-sections for a given ϕ_1^{MN} coordinate value.

For a fixed symbol period T, assume that the average optical power of each transmitted codeword is limited to be at most $P^{\mathsf{G}}/\sqrt{T}$ as defined in (3). In terms of the signal space definition for Υ,

$$\frac{1}{N} \sum_{n=1}^{N} x_{1,n} \leq P^{\mathsf{G}} \quad (5)$$

where $x_{1,n}$ is the coordinate value in the ϕ_1 direction for each constituent symbol. The transmitted NM-dimensional vector $\mathbf{x}$ is taken from the set $\Theta(P^{\mathsf{G}}) = \Upsilon^N \cap \Psi(P^{\mathsf{G}})$ where $\Psi(P^{\mathsf{G}})$ is a hyperplane defined so that the power constraint (5) is satisfied.

B. Set of Received Codewords

For some $\mathbf{x} \in \Theta(P^{\mathsf{G}})$, the received vector, $\mathbf{Y}$ is normally distributed with mean $\mathbf{x}$ and variance equal to the noise variance, σ^2 per dimension. Let Ω_{MN} denote the set of all possible received vectors. By the law of large numbers, with high probability $\mathbf{Y}$ will lie near the surface of a sphere of radius $\sqrt{MN(\sigma^2+\epsilon)}$ where ϵ can be made arbitrarily small by increasing N. A codeword is decoded by assigning all vectors contained inside the sphere to the given codeword.

Let the region $\Omega_\infty = \lim_{N\to\infty} \Omega_{MN}$. This asymptotic set can be formally represented as

$$\begin{aligned} \Omega_\infty &= \{\mathbf{x} + \mathbf{b} : \mathbf{x} \in \Theta(P^{\mathsf{G}}),\ \mathbf{b} \in \rho B^{MN}\} \\ &= \Theta(P^{\mathsf{G}}) \oplus \rho B^{MN} && (6) \end{aligned}$$

where

$$\rho = \sqrt{MN\sigma^2}, \quad (7)$$

the $\oplus$ operation is the *Minkowski addition* of two sets and B^{MN} is the MN-dimensional unit ball. Since $\Theta(P^{\mathsf{G}})$ is convex, Ω_∞ is a parallel convex set of radius ρ, that is, the set of all points with distance at most ρ from $\Theta(P^{\mathsf{G}})$.

Clearly, $\Theta(P^{\mathsf{G}}) \subset \Omega_\infty$ since $\mathbf{0} \in B^{MN}$. Where ever the boundary of $\Theta(P^{\mathsf{G}})$ is smooth, the boundary points of Ω_∞ are a subset of the points parallel to $\Theta(P^{\mathsf{G}})$ at distance ρ away. Form the parallel extension of $\Theta(P^{\mathsf{G}})$ as the region $\Theta(P^{\mathsf{G}}+p_\rho)-h$, for some $h, p_\rho > 0$ as the set of points which are at most distance of ρ away from $\Theta(P^{\mathsf{G}})$ whenever the boundary of $\Theta(P^{\mathsf{G}})$ is smooth. At points of discontinuity, that is, in the "corners" of the bodies in question, the points in Ω_∞ lie inside the parallel extension of $\Theta(P^{\mathsf{G}})$ at a distance ρ away due to the triangle inequality. In other words,

$$\Theta(P^{\mathsf{G}}) \subset \Omega_\infty \subset \Theta(P^{\mathsf{G}} + p_\rho) - h. \quad (8)$$

Let $V(\cdot)$ evaluate to the volume of the region. Since all the regions are closed, an upperbound on $V(\Omega_\infty)$ can be found using (8) to give,

$$V(\Theta(P^{\mathsf{G}} + p_\rho)) > V(\Omega_\infty) > V(\Theta(P^{\mathsf{G}})).$$

By exploiting the geometry of the regions, it is possible to show that for large N, $p_\rho = 2\sigma\sqrt{M}$ to give

$$V(\Theta(P^{\mathsf{G}}+p_\rho)) = V(\Upsilon_1)^N \frac{(M-1)!^N}{(MN)!} (N(P^{\mathsf{G}}+2\sigma\sqrt{M}))^{MN}. \quad (9)$$

C. Upperbound Computation

The channel capacity in bits/symbol can be upperbounded using the sphere packing argument developed for electrical power constrained channels [8]. The maximum rate is upperbounded by the asymptotic number of non-overlapping spheres that can be packed in Ω_{MN} as N goes to infinity. Using the previously defined regions,

$$\begin{aligned} C_{\text{sym}} &\leq \lim_{N\to\infty} \frac{1}{N} \log_2 \frac{V(\Omega_{MN})}{V(\rho B^{MN})} \\ &\leq \lim_{N\to\infty} \frac{1}{N} \log_2 \frac{V(\Theta(P^{\mathsf{G}} + p_\rho))}{V(\rho B^{MN})} \end{aligned} \tag{10}$$

where the volume of the MN-ball can be written as

$$V(\rho B^{MN}) = \frac{\pi^{MN/2}\rho^{MN}}{(MN/2)!}.$$

Using (9) and taking the limit the capacity of the channel can be upperbounded as

$$\begin{aligned} C_{\text{sym}} \leq\ & M \log_2 \left[\left(\sqrt{T}\frac{rP}{\sigma} + 2\sqrt{M} \right) \right. \\ & \left. \frac{V(\Upsilon_1)^{1/M}(M-1)!^{1/M}}{M} \sqrt{\frac{e}{2\pi}} \right] \end{aligned} \tag{11}$$

in units of bits/symbol for some symbol period T.

V. Lowerbound on Channel Capacity

A lower bound on the capacity of the optical intensity channel can be found by computing the mutual information between the channel input and output for any input distribution. An asymptotically tight lower bound for high optical SNR can be achieved if the maxentropic source distribution, subject to an average optical power constraint, is used to compute this lower bound. It is possible to show that this choice of source distribution causes the upperbound (11) and lower bound to converge at high optical SNR.

Due to the signal space definition, the average optical power depends solely on the ϕ_1 coordinate and can be represented as in (2). By the maximum entropy principle, the maxentropic source distribution subject to this constraint must take the form $f^*_{\mathbf{X}}(\mathbf{x}) = K\exp(-\lambda x_1)$, for $\mathbf{x} \in \Upsilon$ and for some $K, \lambda > 0$ [9]. The constants K and λ can be found by using the form of the distribution and solving the following

$$\int_{\mathbf{x}\in\Upsilon} f^*_{\mathbf{X}}(\mathbf{x})d\mathbf{x} = 1$$

$$\int_{\mathbf{x}\in\Upsilon} x_1 f^*_{\mathbf{X}}(\mathbf{x})d\mathbf{x} = P^{\mathsf{G}}$$

to yield

$$f^*_{\mathbf{X}}(\mathbf{x}) = \left(\frac{M}{P^{\mathsf{G}}}\right)^M \frac{1}{V(\Upsilon_1)(M-1)!} \exp\left(-M\frac{x_1}{P^{\mathsf{G}}}\right) \tag{12}$$

for $\mathbf{x} = (x_1, x_2, \ldots, x_M) \in \Upsilon$. Notice that $f^*_{\mathbf{X}}(\mathbf{x})$ is a function of solely the coordinate in the ϕ_1 direction which represents the average optical power of each symbol. The conditional distribution for a given $x_1 = k$ is uniform over all elements of Υ_k, which is entropy maximizing in the absence of constraints.

VI. Bandwidth Constraint on Signal Space Dimension

Previous results with rectangular pulses on the photon counting channel demonstrated that the rate is unbounded if the average optical power is the only constraint [1, 2]. Indeed, it is possible to show that signalling with arbitrarily narrow rectangular pulses in a symbol interval of T at a given average optical power causes the upperbound in (11) to tend to infinity.

However, previous work on the photon counting channel also indicated that this unbounded rate necessarily comes at the price of an infinite bandwidth requirement [5]. It is clear that in order to have a consistent bound or notion of maximum rate for this channel that a bandwidth constraint must be placed on the space of signals transmitted.

Imposing a bandwidth constraint on a set of time-limited signals is not straight forward since the Fourier spectrum is necessarily time-unlimited. Define the fractional power bandwidth, W_K, of a transmitted symbol $x(t)$ with Fourier transform $X(f)$ as

$$\frac{\int_{-W_K}^{W_K} |X(f)|^2 df}{\int_{-\infty}^{\infty} |X(f)|^2 df} = K$$

where $K \in (0, 1)$ is fixed to some value typically 0.99 or 0.999. The orthonormal family of prolate spheroidal wave functions are time-limited functions which have for a given K the minimum W_K of all unit energy functions with support in $[0, T)$ [10–12]. For signals $x(t)$, approximately $\kappa = 2W_K T$ prolate spheroidal wave functions are required to represent the function with an error that tends to zero as $K \to 1$. Thus, κ can be regarded as the "essential" dimension of the set of signals time-limited to $[0, T)$ with fractional power bandwidth W_K.

In order to bound the maximum rate possible, select the the effective dimension value κ over all symbols in Υ so that the rate is maximized. In light of the spectral constraint, the capacity of the channel is expressed as a maximum spectral efficiency in units of bits/second/Hertz, C_η as opposed to C_{sym} in (11) which is in units of bits/symbol. Spectral efficiency is a more appropriate measure of the rate of since it combines important practical channel performance measures of data rate and bandwidth. Thus the upperbound on channel capacity in (11) can be represented as a bound on the maximum spectral efficiency using the effective dimension κ and (3) as,

$$\begin{aligned} C_\eta \leq\ & \frac{2M}{\kappa} \log_2 \left[\left(\sqrt{\frac{\kappa}{2W_K}}\frac{rP}{\sigma} + 2\sqrt{M} \right) \right. \\ & \left. \frac{V(\Upsilon_1)^{1/M}(M-1)!^{1/M}}{M} \sqrt{\frac{e}{2\pi}} \right] \end{aligned} \tag{13}$$

in units of bits/second/Hertz. Unlike the bandlimited case where the dimension of each basis signal is one, here the

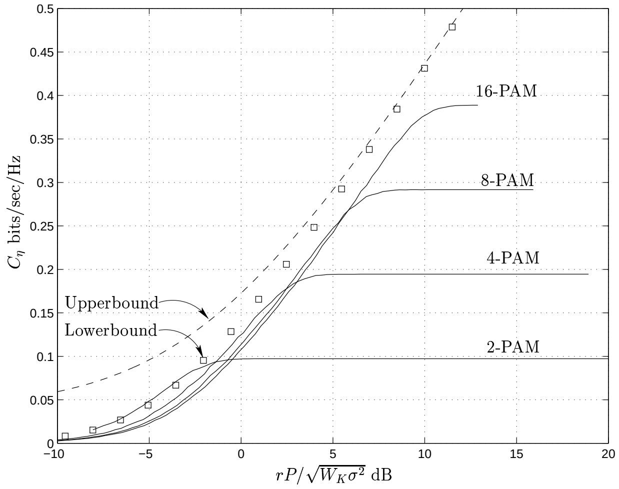

Fig. 1. Bounds on the achievable spectral efficiencies using rectangular PAM along with results for some uniform discrete constellations.

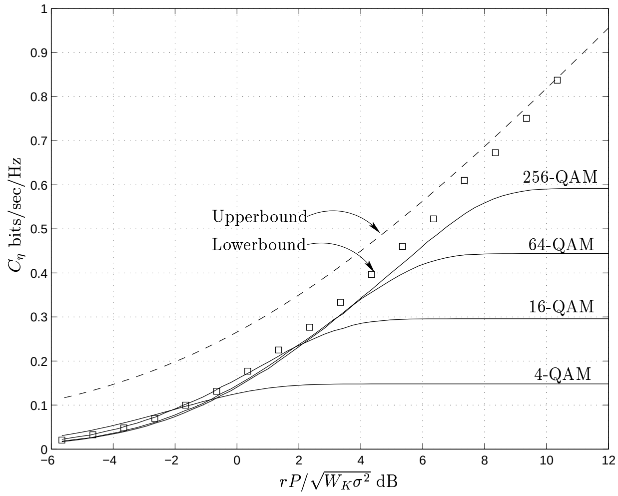

Fig. 2. Bounds on the achievable spectral efficiencies using optical intensity raised-QAM along with results for some uniform discrete constellations.

dimension of each signal in the constituent constellation must be computed. Define κ as the effective dimension of signalling scheme as the maximum effective dimension over all transmit symbols. In this manner, every signal in the constellation can be represented in a κ dimensional space, where some coordinates may be zero.

At high optical SNRs, the lower bound on capacity tends to the true capacity since it is chosen to be the maxentropic source distribution. It is possible to show that using this bandwidth constraint the upper and lower capacity bounds converge at high optical signal-to-noise ratios. As a result, we make the claim that the upper and lower capacity bounds computed here are asymptotically exact.

VII. Examples and Discussion

A. PAM

Form an M-ary pulse-amplitude modulation scheme using the rectangular pulse shape of (1). Define the effective dimension of the scheme using the 99% fractional power bandwidth (K=0.99) to yield $\kappa_{\mathrm{PAM}} = 20.572$.

Figure 1 presents the upper and the lower bounds on C_η for the PAM scheme defined as well as spectral efficiency curves for for discrete uniform 2, 4, 8 and 16 point constellations versus optical SNR. These spectral efficiency curves were computed numerically using Monte Carlo methods.

The upper bound on capacity is obtained by direct application of (13) to give,

$$C_\eta^{\mathrm{PAM}} \le \frac{2}{\kappa}\log_2\left[\left(\sqrt{\frac{\kappa}{2W}}\frac{rP}{\sigma}+2\right)\sqrt{\frac{e}{2\pi}}\right].$$

The lower bound on capacity was determined first by computing $f_{\mathbf{Y}}(\mathbf{y})$, which takes the form

$$\begin{aligned} f_{\mathbf{Y}}(\mathbf{y}) &= f^*_{\mathbf{X}}(\mathbf{x}) * f_{\mathbf{Z}}(\mathbf{z}) \\ &= \frac{1}{P^{\mathsf{G}}}\left(1-Q\left(\frac{y}{\sigma}-\frac{\sigma}{P^{\mathsf{G}}}\right)\right)\exp\left(\frac{\sigma^2-2y}{2P^{\mathsf{G}}}\right) \end{aligned}$$

where $Q(x) \triangleq (1/\sqrt{2\pi})\int_x^\infty \exp(-u^2/2)du$. Since $f_{\mathbf{Y}}(\mathbf{y})$ does not have a closed form in this case, computing the mutual information explicitly is impossible. Figure 1 shows the lower bound computed for a number of points. Note that at high SNR the lower and upper bounds on capacity approach one another.

B. Raised-QAM

An optical 3-dimensional raised-QAM scheme can be defined by specifying $\phi_1(t)$ as in (1) and

$$\begin{aligned} \phi_2(t) &= \sqrt{\frac{2}{T}}\cos(2\pi t/T) \\ \phi_3(t) &= \sqrt{\frac{2}{T}}\sin(2\pi t/T) \end{aligned}$$

for $t \in [0,T)$ [7]. Figure 2 presents a plot of the upper bound on capacity (13) for a 3-dimensional raised-QAM scheme which takes the form

$$C_\eta^{\mathrm{QAM}} \le \frac{6}{\kappa}\log_2\left[\left(\sqrt{\frac{\kappa}{2W}}\frac{rP}{\sigma}+2\sqrt{3}\right)\sqrt{\frac{e}{18\pi^{1/3}}}\right].$$

Using the same definition of bandwidth, $K = 0.99$, $\kappa_{\mathrm{QAM}} = 27.038$. As is the case with PAM, the lower bound must be computed numerically. Unfortunately, computation of $f_{\mathbf{Y}}(\mathbf{y})$ is difficult and the lower bound was computed using a discretized version of $f^*_{\mathbf{X}}(\mathbf{x})$ (12) and integrated using Monte Carlo methods. The upper and lower bounds approach one another at high optical SNRs Spectral efficiency curves for 4, 16, 64 and 256 point uniform distributions were determined using Monte Carlo techniques and are also presented.

C. Discussion

An important difference over the electrical channels is that the upper and the lower bound depend explicitly on the pulse set chosen. Thus, C_η is a measure of the maximum spectral efficiency of the optical channel for the given

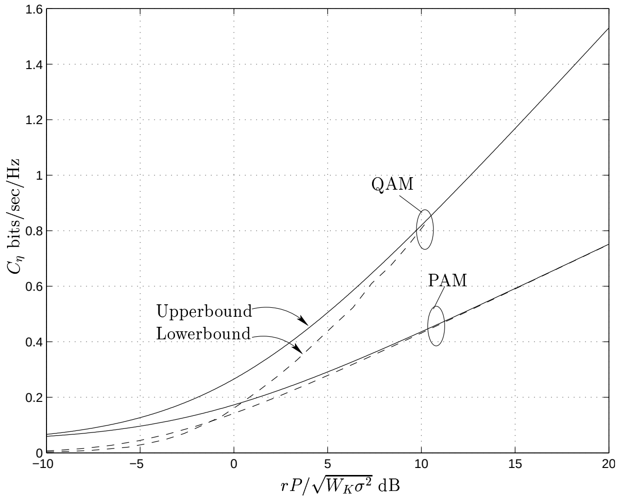

Fig. 3. Comparison of achievable spectral efficiencies using rectangular PAM versus optical intensity raised-QAM.

pulse set. Indeed, in order to determine a bound on the maximum spectral efficiency, C_η should be maximized over all intensity pulse sets, that is, over all Υ. Some early work on the photon counting channel demonstrated that narrow pulse position techniques were optimal pulse techniques in the sense of a given average distance measure [13, 14]. Capacity results for the photon counting channel nearly exclusively assume that rectangular pulse techniques are employed. Here the assumption on the shape of the pulses is removed and the maximum spectral efficiencies are computed for a given pulse set. However, the rate maximizing pulse set for an optical intensity channel under an average optical and bandwidth constraint is an open problem.

At high optical signal-to-noise ratios, pulse techniques have lower maximum spectral efficiencies than bandwidth efficient techniques. Figure 3 presents a comparison of the capacity bounds derived earlier. Note that at high SNRs signalling schemes based on the raised-QAM pulse set have nearly twice the maximum spectral efficiency of the rectangular PAM techniques at a given SNR. At lower optical SNR, the derived bounds are loose and do not reveal any new insight. Indeed, at low SNR, when the available spectral efficiencies tend to zero, rectangular pulse techniques are attractive due to their ease of implementation.

VIII. Conclusions

We have derived capacity bounds for the optical intensity channel with average optical power and bandwidth constraints in Gaussian noise. These results complement rather than contradict previous work on the Poisson photon counting channel. The photon counting channel can be viewed as an optical system operating at low optical power where the quantum nature of the photons dominates performance. Rectangular pulse techniques are uniquely considered since the bandwidth of the channel is considered to be very large.

In this work, we treat a fundamentally different channel. Indoor free-space channels suffer from reduced bandwidth due to multipath distortion and from white, Gaussian noise due to high background illumination. The derived capacity bounds are not restricted to pulse techniques, as in previous work, but are general and treat all time-disjoint optical intensity schemes. A bandwidth constraint is imposed on the set of signals that are transmitted by way of determining the effective dimension of the space of time-limited signals with a given fractional power bandwidth. The derived capacity bounds demonstrate that for a given average optical power, pulse techniques have significantly lower maximum spectral efficiencies than bandwidth efficient techniques. In particular, significant rate gains can be had by using a raised-QAM pulse set over a rectangular PAM at high optical signal-to-noise ratios.

References

[1] J. P. Gordon, "Quantum effects in communication systems," *Proc. IRE*, pp. 1898–1908, September 1962.
[2] J. R. Pierce, "Optical channels: Practical limits with photon counting," *IEEE Trans. Commun.*, vol. COM-26, no. 12, pp. 1819–1821, December 1978.
[3] M. H. A. Davis, "Capacity and cutoff rate for Poisson-type channels," *IEEE Trans. Inform. Theory*, vol. IT-26, no. 6, pp. 710–715, November 1980.
[4] A. D. Wyner, "Capacity and error exponent for the direct detection photon channel — Part I and II," *IEEE Trans. Inform. Theory*, vol. 34, no. 6, pp. 1449–1471, November 1988.
[5] R. J. McEliece, "Practical codes for photon communication," *IEEE Trans. Inform. Theory*, vol. IT-27, no. 4, pp. 393–398, July 1981.
[6] J. M. Kahn and J. R. Barry, "Wireless infrared communications," *Proc. IEEE*, vol. 85, no. 2, pp. 263–298, February 1997.
[7] S. Hranilovic and F. R. Kschischang, "Lattice codes for optical intensity modulated, direct-detection channels using time-disjoint symbols," *IEEE Trans. Inform. Theory*, submitted for publication, September 6, 2001. Available online at `http://www.comm.utoronto.ca/~steve`.
[8] C. E. Shannon, "Communication in the presence of noise," *Proc. IRE*, vol. 37, no. 1, pp. 10–21, January 1949.
[9] T. M. Cover and J. A. Thomas, *Elements of Information Theory*, Wiley & Sons Publishers, New York, NY, 1991.
[10] B. Slepian and H. O. Pollak, "Prolate spheroidal wave functions, Fourier analysis and uncertainty – I," *Bell Syst. Techn. J.*, pp. 43–63, January 1961.
[11] H. J. Landau and H. O. Pollak, "Prolate spheroidal wave functions, Fourier analysis and uncertainty – II," *Bell Syst. Techn. J.*, pp. 65–84, January 1962.
[12] H. J. Landau and H. O. Pollak, "Prolate spheroidal wave functions, Fourier analysis and uncertainty – III: The dimension of the space of essentially time- and band-limited signals," *Bell Syst. Techn. J.*, pp. 1295–1336, July 1962.
[13] B. Reiffen and H. Sherman, "An optimum demodulator for Poisson processes: Photon source detectors," *Proc. IEEE*, vol. 51, pp. 1316–1320, October 1963.
[14] K. Abend, "Optimum photon detection," *IEEE Trans. Inform. Theory*, vol. 12, no. 1, pp. 64–65, January 1966.